

## As-Cast Titanium Aluminides Microstructure Modification

*A. Duarte, F. Viana, Henrique M.C.M. Santos*

*GMM/IMAT, Departamento de Engenharia Metalúrgica e de Materiais, FEUP  
Rua dos Bragas, 4099 Porto Codex, Portugal*

Received: August 15, 1998; Revised: March 30, 1999

Two cast  $\gamma$  titanium aluminides, Ti47Al and Ti50Al (at. %), were obtained by arc melting under an argon atmosphere. The as-cast microstructure modification by annealing under protective argon atmosphere and hot isostatic pressing (HIP) was analysed by optical and scanning electron microscopy with microanalysis facilities. As-cast structures presented strong microsegregations, being composed of primary  $\alpha$  dendrites (with low Al content), which transformed into lamellar  $\alpha_2 + \gamma$  during solid state cooling, and interdendritic  $\gamma$  phase (with high Al content). Annealing in the  $\alpha + \gamma$  field was responsible for a partial reduction of microsegregation, a decreasing of the volume fraction of  $\alpha_2 + \gamma$  lamellar dendrites, an increasing of  $\gamma$  volume fraction and the occurrence of a small fraction of  $\alpha_2$  particles and plates in some of the  $\gamma$  grains. Annealing in the  $\alpha$  field at 1400 °C for one hour was insufficient to eliminate the as-cast microstructure in the Ti50Al alloy and produced large equiaxed lamellar colonies of  $\alpha_2 + \gamma$  in the Ti47Al alloy. HIP in the  $\alpha + \gamma$  field (to avoid excessive grain growth) was responsible for microstructure modifications similar to the ones obtained by heat treating under similar soaking conditions.

**Keywords:** *titanium aluminides, microstructure, heat treatment*

### 1. Introduction

Titanium aluminides with low density, oxidation resistance up to 800 °C and good creep resistance are promising alloys for high temperature structural applications, the lack of room temperature ductility being the main obstacle to its utilization as engineering materials<sup>1,2</sup>.

Mechanical properties of these alloys are strongly microstructure dependent. Structures with fine mixtures of  $\gamma$  grains and  $\alpha_2$  plates or particles, called “duplex” or “near-gamma”, conduct to a reasonable balance of properties but at relatively low levels; refined lamellar structures are responsible for properties, up to 760 °C, comparable or better than those of Ni-based superalloys. Several  $\gamma$ -TiAl based alloys with small amounts of refractory elements, for increased high temperature properties, and grain refiners have been studied to attain well-balanced room temperature ductility and high temperature strength<sup>1</sup>.

The solidification of these alloys, accordingly to the phase diagram, occurs through two peritectic reactions,  $L + \beta \rightarrow \alpha$  and  $L + \alpha \rightarrow \gamma$ , that will hardly be complete due to limited diffusion caused by the formation of a solid envelope of the peritectic phase, avoiding the physical contact between the reactants. For both peritectic reactions,

high cooling rates or melt undercooling inhibit the formation of the pro-peritectic solid phase; the incompleteness of the peritectic reactions will cause the remaining liquid to progressively enrich in aluminium and solidify, at lower temperatures, as interdendritic  $\gamma$  phase. The as-cast structure presents strong microsegregation and texture needing thermomechanical treatments to be eliminated<sup>3,4,5</sup>. Microsegregation is responsible for aluminium contents varying from 44.7 at. % in  $\alpha_2 + \gamma$  dendrites to 48.9 at. % in interdendritic  $\gamma$  for a Ti48Al2Cr2Nb alloy<sup>4</sup>, while these figures attain 51 and 56 %, respectively, for a Ti50Al alloy<sup>3</sup>. During solid state cooling  $\alpha$ -dendrites (hcp structure) transform into lamellar structures, composed of  $\alpha + \gamma$  phases (this last phase has an ordered fct - L1<sub>0</sub> structure) and, at lower temperatures, to  $\alpha_2 + \gamma$  phases ( $\alpha_2$  has an ordered hcp - DO<sub>19</sub> structure)<sup>3,6,7</sup>.

Homogenizing treatments conducted in the  $\alpha + \gamma$  field are generally inefficient, higher temperatures, in the  $\alpha$  field, being usually needed<sup>8</sup>. Treatments in the  $\alpha$  field are responsible for excessive grain growth, so the temperature has to be kept low<sup>9</sup>. Microstructures obtained after cooling from the  $\alpha$  phase field are sensitive to the cooling rate: low cooling rates, typically in the furnace, lead to lamellar

structures with  $\alpha_2$  and  $\gamma$  lamellae; higher cooling rates are responsible for a Widmanstätten structure;  $\alpha$  to  $\gamma$  massive transformation results from even higher cooling rates. The  $\gamma$ -massive transformation nucleates at  $\alpha$  grain boundaries and progresses to the grain interior; for a high cooling rate and/or coarse grain size the transformation may be incomplete and the grain interiors are not transformed<sup>6,7,10,11</sup>. For Ti47.5Al and Ti48Al alloys the non transformed areas present very fine lamellae of  $\alpha_2$  and  $\gamma$ ; these lamellae are similar to the ones presented by a brine cooled totally  $\alpha$  structure Ti40Al after annealing in the  $\alpha + \gamma$  field<sup>7,11,12</sup>.

The fine lamellar structures are quite different from the coarser ones resulting from slow cooling rates. These are more stable than the fine ones and when heated to 1000 °C coarsen by fragmentation of some lamellae and thickening at the expenses of others that dissolve and  $\gamma$  grains will form at lamellar colony boundaries. If the temperature is raised to 1200 °C, interlamellar spacing increases and coarse  $\alpha_2$  particles and plates are present at non lamellar  $\gamma$  grains<sup>13</sup>.

## 2. Materials and Procedures

In this work two titanium aluminides were produced, Ti50Al and Ti47Al (hereafter all compositions are given in atomic percentage), by the arc melting technique under argon atmosphere in a water cooled copper mould. The raw

materials used were Ti and Al high purity bars. A previous casting procedure was established in order to obtain as-cast materials free from macro-segregation, with some ten grams of weight and 14 mm diameter.

HIP was conducted in argon atmosphere at a temperature of 1250 °C during 4 h, under a pressure of about 180 MPa. Alternatively heat treatments were carried out on as-cast aluminides, under a protective argon flux. The samples were submitted to a set of heat treatment cycles. The pre-heating of 10 min at 800 °C was followed by a 10 °C/min heating rate until the maximum temperatures of 1150, 1250, 1350 and 1400 °C for a maximum stage of 6 h. A longer cycle was tested at 1250 °C during 36 h for the Ti50Al alloy. All the samples were cooled inside the furnace, at an average rate of 12 °C/min from the maximum temperature to 900 °C.

The as-cast aluminides chemical compositions of Ti and Al were evaluated using 4 different techniques: energy dispersion spectrometry (EDS), wavelength dispersion spectrometry, inductive coupled plasma, and atomic absorption spectrometry. Similar results were achieved independently of the technique used; the variation around nominal compositions is  $\pm 0.2$  at. %. To measure phase chemical compositions the quantitative EDS analysis with standards of pure Al and Ti (FIROZ corrected) was performed in the scanning electron microscope (SEM) Jeol JSM 35 C. The accuracy of measurements is  $\pm 0.5$  at. %.

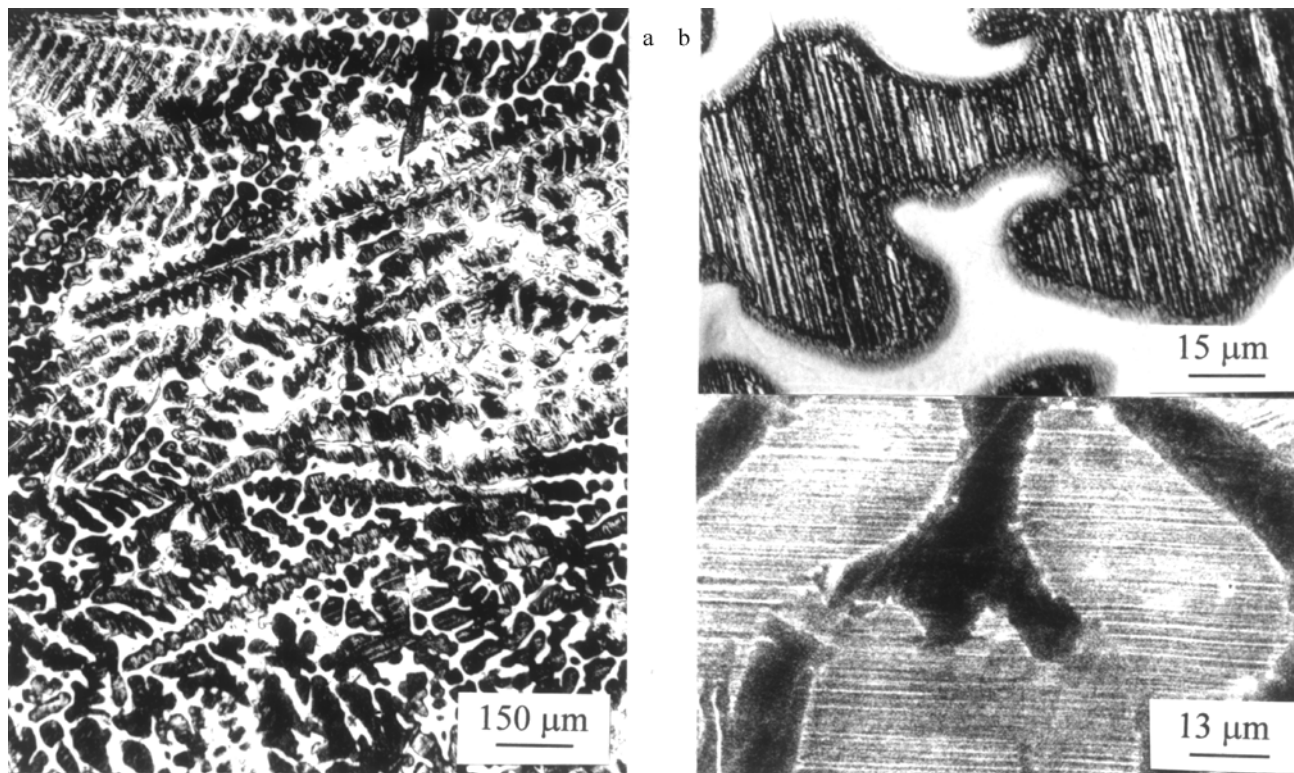


**Figure 1.** Optical microstructures of the as-cast Ti50Al alloy (a) and (b) and SEM under atomic number contrast (c).

**Table 1.** Chemical composition of the as-cast materials, determined by EDS.

Region analysed	Chemical composition (at. %)			
	Ti50Al		Ti47Al	
	Ti	Al	Ti	Al
Lamellar structure	52.0 - 53.6	46.4 - 48.0	not available	not available
Bright lamellar structure	not available	not available	53.9 - 54.9	45.1 - 46.1
Dark lamellar structure	not available	not available	50.1 - 51.2	48.8 - 49.9
$\gamma$ -Phase	46.0 - 46.6	53.4 - 54.0	47.7	52.3

Samples not etched were SEM observed under an atomic number contrast.

The samples for optical microscopy (OM) and SEM observation were prepared following standard metallographic techniques proposed by Ref. 14. The OM studies used differential interferential contrast and Kroll's solution as the etching reagent.

As-cast and HIPed densities were investigated using the Micromeritics Accupyc 1330 pycnometer with 0.001 measurement precision.

### 3. Results and Discussion

#### 3.1. As-cast structure characterization

The optical microstructure of the as-cast Ti50Al alloy presents long dark dendrites and a white interdendritic phase - see Fig. 1 a. Higher magnifications resolve the lamellar nature of the dendritic areas - see Fig. 1 b. SEM observations under atomic number contrast reveal a different chemical composition for the lamellae, with an average Al content of 46.4 to 48.0% - see Table 1; the interdendritic phase has a higher Al content, from 53.4 to 54.0%. Accordingly to the phase diagram<sup>15</sup>, a Ti50Al alloy should complete the solidification with  $\alpha$  dendritic structure; the occurrence of the interdendritic phase requires coring during  $\alpha$  formation, with consequent Al enrichment of the liquid, which will finally solidify as  $\gamma$  phase as reported by

Ref. 3. The  $\alpha$  dendrites transform into  $\alpha_2 + \gamma$  lamellae during solid state cooling and the  $\gamma$  phase remains interdendritic.

The phase diagram shows that a decrease in Al content of the alloy implies a progressively higher fraction of  $\alpha$  phase after solidification, but even for the Ti47Al alloy the interdendritic  $\gamma$  remains in the as-cast structure, enhancing the intensity of the segregation - see Fig. 2. In the lamellar structure a higher aluminium content (see Table 1) has been evaluated in regions near the interdendritic phase, the darker lamellar areas in Fig. 2b. All these features support the assumed coring hypothesis.

#### 3.2. Heat treatment structure characterization

The characteristic microstructures obtained by heat treating Ti50Al in the  $\alpha + \gamma$  field are shown in the Figs. 3 and 4. In the SEM microstructures shown in Fig. 3 the following constituents are identified:  $\gamma$ -phase (dark regions);  $\alpha_2$  (thicker white regions); and lamellar structure, remaining from dendrites. It is clear that the dendritic fraction after 6 h at 1250 °C has decreased, showing that solution of  $\alpha_2 + \gamma$  dendrites has progressed; even after an increased stage of 36 h the  $\alpha_2$  phase is still present - see Fig. 4a. The phase diagram states that at this temperature a totally  $\gamma$  structure should be obtained, so equilibrium structure has not been reached. Increasing the temperature to 1350 °C for 6 h or 1400 °C for 1 h resulted in a dendritic fraction smaller than the one obtained for the 6 h treatment

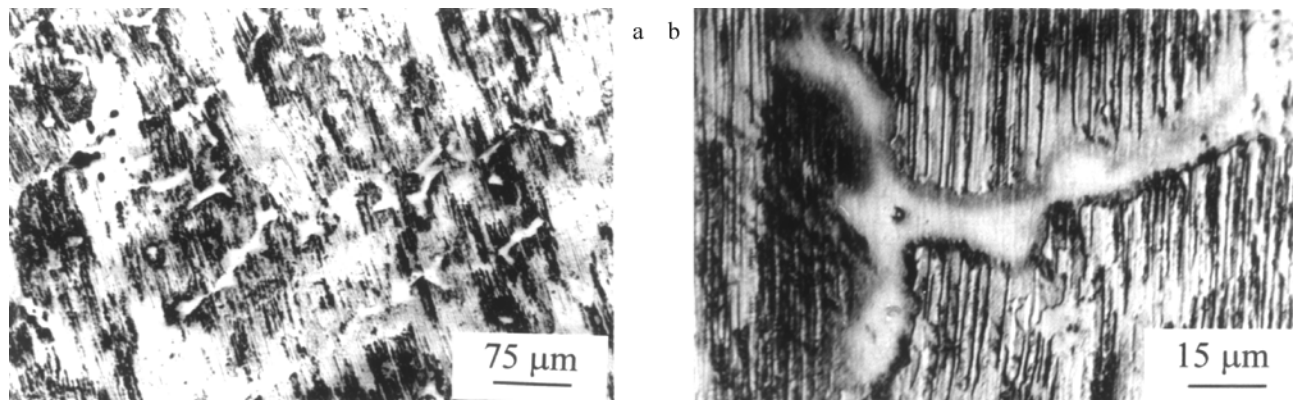


**Figure 2.** Optical micrographs of the as-cast Ti47Al alloy.

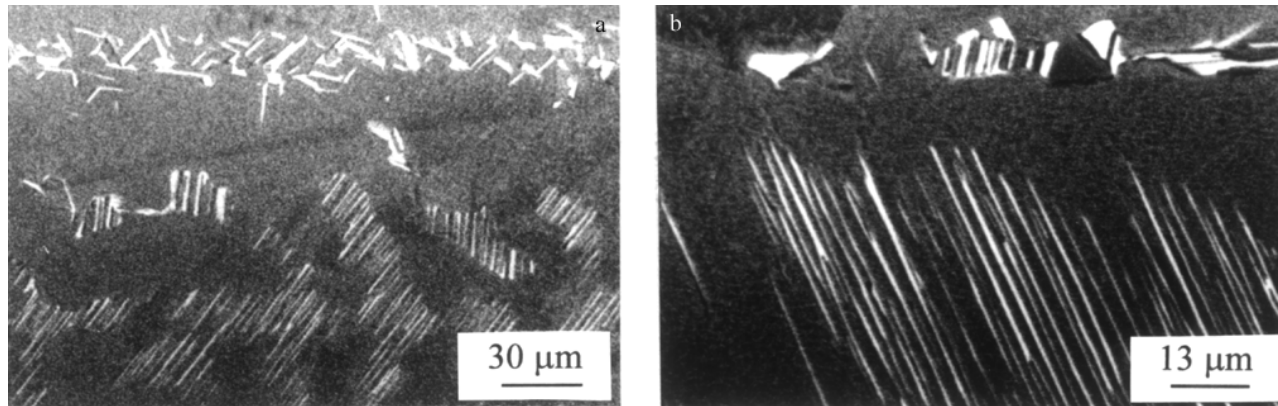


**Figure 3.** SEM micrographs of Ti50Al heat treated at 1250 °C during 6 h.

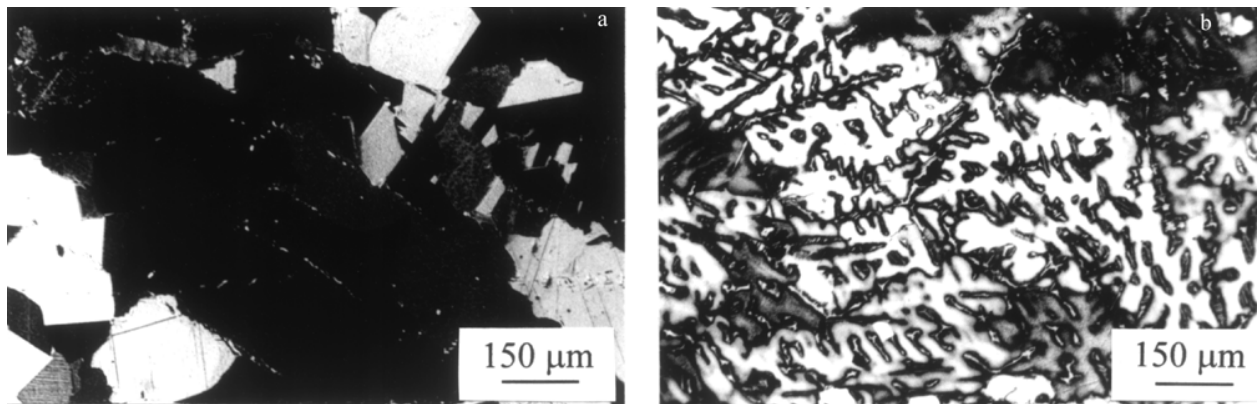


**Figure 4.** Optical micrographs of heat treated Ti50Al at 1250 °C for 36 h (a) and at 1400 °C for 1 h (b).

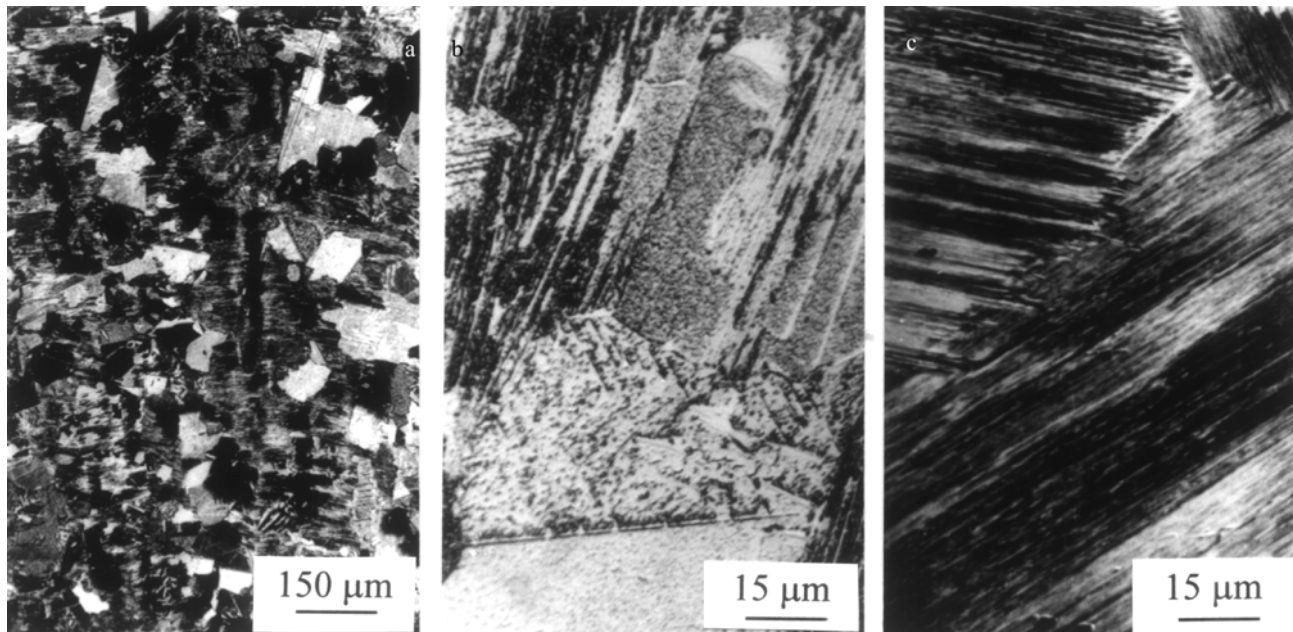


**Figure 5.** Optical micrographs of heat treated Ti47Al at 1250 °C for 6 h (a) and (b), and at 1400 °C for 1 h (c).

at 1250 °C (see Fig. 4b). Microanalysis measurements reinforce the microstructural observations:  $\gamma$  phase decreases its Al content and lamellar structure becomes richer (see Table 2), approaching equilibrium.

Figure 5 illustrates the dendritic structure attenuation for Ti47Al, along with the  $\gamma$  phase formation. The microstructures of samples treated in  $\alpha + \gamma$  field - see Figs. 5a and b - reveal a matrix of  $\gamma$ -phase and lamellar grains, duplex

**Table 2.** Al content of the heat treated materials, determined by EDS.

Region	Ti50Al		
	1250 °C 6 h	1250 °C 36 h	1400 °C 1 h
analysed			
$\gamma$ -Phase	50.2 – 51.1	48.3 - 49.5	48.8 - 51.1
$\alpha_2$ -phase	39.0	not available	41.1
Lamellar structure	48.8	not available	48.6

likely, and a few number of  $\alpha_2$  dispersed particles are also observed. One  $\alpha$  phase field treatment produced a fully-lamellar structure represented in the Fig. 5 c; dendrites are no longer visible after this treatment which may be supposed as capable of producing an equilibrium state, causing a totally  $\alpha$  structure after the isothermal stage. The lamellar colony size after this treatment is very high, in agreement with the literature<sup>9,13</sup>; the minimum colony size measurement was 2 mm.

### 3.3. Hip structure characterization

HIPed microstructure of Ti50Al can not be distinguished from the one obtained by heat treatment, for similar soaking conditions, in terms of both phase transformation and chemical composition analysis. The measured rate of densification obtained by the HIP process (0.5%) is in the limit of the resolution of the equipment used and should be carefully considered.

## 4. Conclusions

From this work the following conclusions are withdrawn:

- i) as-cast structures of arc-melted Ti50Al and Ti47Al present strong microsegregation, revealed by the systematic occurrence of interdendritic  $\gamma$  phase;
- ii) the efficiency of the homogenizing treatment applied to the as-cast structure of Ti50Al alloy is low; even after high temperatures and long times (1250 °C for 36 h and 1400 °C for 1 h) primary dendrites remain visible;
- iii) as-cast structure of Ti47Al alloy has been destroyed by an  $\alpha$  field treatment (1400 °C for 1 h), although an ultra coarse fully lamellar structure resulted;

iv) HIP microstructure modifications are close to the ones obtained from similar heat treatment conditions.

## Acknowledgments

This work was supported by PRAXIS XXI project with reference 3/3.1/CTAE/1904/95. A grant BIC 3621 from PRAXIS XXI was conceded to A. Duarte to cooperate in this project.

## References

1. Kim, Y.-W.; Dimiduk, D.M. *Structural Intermetallics 1997*, Nathal, M.V. *et al.*, eds., TMS, 531, 1997.
2. Froes, F.H.; Suryanarayana, C.; Eliezer, D. *J. Mat. Sci.*, n. 27, p. 5113, 1992.
3. Shao, G.; Tsakirooulos, P.; Miodownik, A.P. *Mat. Sci. and Techn.*, n. 13, p. 797, 1997.
4. Muraleedharan, K.; Rishel, L.L.; De Graef, M.; Cramb, A.W.; Pollock, T.M.; Gray III, G.T. *ibid*, n. 1, p. 215.
5. Naka, S.; Thomas, M.; Sanchez, C.; Khan, T. *ibid*, n. 1, p. 313.
6. Kumagai, T.; Abe, E.; Nakamura, M. *Metall. and Mat. Trans. A*, n. 29A, p. 19, 1998.
7. Veeraraghavan, D.; Ramanath, G.; Wang, P.; Vasudevan, V.K. *Solid → Solid Phase Transformations*, Jonhson, W.C., *et al.*, eds., TMS, 273 (1994).
8. Semiatin, S.L.; Chesnutt, J.C.; Austin, C.; Seetharaman, V. *ibid*, n. 1, p. 263.
9. Zhang, W.J.; Francesconi, L.; Evangelista, E. *Mat. Letters*, n. 27, p. 135, 1996.
10. Ramanujan, R.V. *ibid*, n. 7, p. 881.
11. Abe, E.; Kumagai, T.; Nakamura, M. *ibid*, n. 1, p. 167.
12. Nakai, K.; Ono, T.; Ohtsubo, H.; Ohmori, Y. *Mat. Trans.*, JIM, n. 37, p. 813, 1996.
13. Ramanujan, R.V.; Maziasz, P.J.; Liu, T. *Acta Mat.*, n. 44, p. 2611, 1996.
14. Glatz, W.; Retter, B.; Leonhard, A.; Clemens, H. *Structure*, n. 29, p. 3, 1996
15. McCullough, C.; Valencia, J.J.; Levi, C.G.; Mehrabian, R. *Acta Metall.*, n. 37, p. 1321, 1989.